



Cost-based resilience assessment of bridges subjected to earthquakes

Journal:	<i>International Journal of Disaster Resilience in the Built Environment</i>
Manuscript ID	Draft
Manuscript Type:	Research Paper
Keywords:	Resilience, Earthquakes, Vulnerability, Restoration, Infrastructure, Disaster mitigation

Cost-based resilience assessment of bridges subjected to earthquakes

ABSTRACT

Transport infrastructure resilience is of paramount importance for societies and economies, therefore its quantification is urgently needed. Resilience of infrastructure assets and networks depends on their ability to absorb the actions of natural hazards with minimal loss of functionality, their redundancy for providing alternatives for damaged components and the rapidity of damage restoration. Hence, owners and operators would be benefited in the decision-making process from quantifications of resilience that account for different hazard events, the type and extent of expected damage, the direct and indirect losses and the time of restoration. This paper presents a resilience assessment framework based on well-informed resilience indices, taking into account the abovementioned factors. The framework is applied for assessing the resilience of representative bridges in Thessaloniki, Greece, exposed to earthquakes. The application quantifies the robustness of bridges against different seismic hazard scenarios, by utilizing realistic fragility functions and the rapidity of the recovery and/or retrofitting after the occurrence of a certain degree of damage, based on realistic restoration functions. Two different approaches for the modelling of the restoration tasks are examined. Both direct losses due to structural damage and indirect losses due to traffic disruption are included in the analysis. The results are expected to facilitate owners to enhance cost-based resilience management toward safer and more resilient infrastructure.

Keywords: bridges, resilience, earthquakes, vulnerability, restoration, direct and indirect losses, transport networks

1. Introduction

Bridges are key assets of the transport infrastructure, upon which world economies and societies heavily rely. Recent natural disasters have revealed the vulnerabilities of bridge infrastructure to diverse hazards, e.g. earthquakes, liquefaction, floods or tsunamis, and they had led to significant economic losses and long-term disruptions to the transport network. For example, during the 2009 floods in Cumbria, UK, at least 20 bridges were destroyed or damaged, causing one fatality, £34m of restoration costs and large societal impact (Cumbria County Council, 2010). The impact of seismic ground motion and cascading hazards such as liquefaction, landslides or tsunamis on bridges and transport networks has been also tremendous in past events across the world (Akiyama et al., 2019; Nakanishi et al. 2014). Therefore, assessing the vulnerabilities and quantifying the resilience of bridges and transport networks exposed to natural hazards and in particular, earthquakes and floods, is of paramount importance for the safety and continuity of services, and hence for the growth of economy and the resilience of communities (Rehak et al. 2019; Komendantova et al. 2016). Resilience describes the emergent property or attributes that a bridge or a network has, which allows them to withstand, respond and/or adapt to a vast range of disruptive events by preserving and even enhancing critical functionality (Ayyub, 2014, Elms et al. 2019). Resilience accounts for structural functionality and recovery planning after the occurrence of a hazard, to achieve downtime objectives as defined by the owners or network operators. Metrics of resilience usually measure the quality

38 or performance of the asset or system before and after the event (Hosseini et al., 2016), considering the
39 robustness, redundancy, resourcefulness and rapidity to recovery (Bruneau et al., 2013).

40 In this context, resilience-based design and management are the new principles that are gradually being
41 adopted in practical applications of critical infrastructure and are expected to be incorporated in the next
42 generation of codes, as for example the Resilience-based Earthquake Design Initiative (REDi) for the Next
43 Generation of Buildings (Almufti & Willford, 2013). Risk and resilience assessment frameworks have been
44 proposed for bridges subjected to single hazards (Decò et al., 2013, Bocchini & Frangopol, 2012a) and
45 multiple hazards (Bocchini et al., 2012, Dong & Frangopol 2015, Argyroudis et al., 2020, Banerjee et al.,
46 2019) and for transport networks (Bocchini & Frangopol, 2012b, Zhang et al., 2017, Twumasi-Boakye &
47 Sobanjo, 2018).

48 The resilience assessment frameworks include the characterization of hazard, the vulnerability of the assets
49 and the evaluation of consequences in terms of functionality and repair loss. In some cases, the indirect
50 losses due to traffic disruptions are also accounted in the assessment (Decò et al., 2013, Dong & Frangopol
51 2015, Banerjee et al., 2019). The vulnerability of a bridge under a given hazard can be obtained using
52 fragility functions, which describe the probability of the structure experiencing or exceeding a damage state,
53 for a given intensity measure, e.g. peak ground acceleration (PGA). Available fragility functions for bridges
54 and other transport infrastructure are summarised by Argyroudis et al. (2019), Billah & Alam (2015) and
55 Gidaris et al. (2017). Fragility functions can be derived based on analytical (e.g. Moschonas et al., 2009),
56 empirical (e.g. Basoz et al., 1999; Elnashai et al., 2004) or hybrid approaches for classes of bridges or
57 specific bridges accounting for the effect of geometry, structural system, component and soil properties
58 (Stefanidou & Kappos, 2018). Fragility functions are essential for the estimation of direct, i.e. due to bridge
59 repair, and indirect, i.e. due to loss of bridge functionality, losses. The functionality of the damaged bridge
60 is commonly defined based on engineering judgement (Mackie & Stojadinovic, 2006; FEMA, 2009;
61 Bocchini & Frangopol, 2012a), while the restoration of functionality is usually described through
62 restoration functions, which are necessary for the quantification of resilience and the estimation of the direct
63 and indirect losses. The restoration functions express the rapidity of recovery and they can be expressed by
64 different shapes, such as linear (Chandrasekaran & Banerjee 2016), trigonometric (Cimellaro et al., 2010;
65 Bocchini & Frangopol, 2012a), step-wise (Padgett & DesRoches, 2007; Sharma et al., 2018) or cumulative
66 distribution functions (FEMA, 2009; Bocchini et al., 2012). The restoration process depends on the type of
67 asset, the damage level, the availability of resources and the prioritization of the owner's goals (Hayat et
68 al. 2019).

69 The novelty of this paper is the delivery of well-thought restoration functions for three very common
70 highway bridges, for which alternative approaches for expressing the restoration strategies were examined
71 and assessed with regard to their practicality. In this context, a typical risk and resilience assessment
72 framework is employed to these representative bridges, which lie along the Ring Road of Thessaloniki,
73 Greece, considering exposure and damages to earthquake hazards. The vulnerability of the bridges against
74 different seismic scenarios is quantified by utilizing realistic fragility functions and the rapidity of the

1
2
3 75 recovery after the occurrence of a certain degree of damage is estimated based on realistic restoration
4 76 functions. The restoration process is modelled accounting for realistic and representative restoration tasks
5 77 of the damaged bridge components, considering the post-disaster idle time and the repair duration
6 78 variability. Two different restoration models are examined: a linear (deterministic) as per FEMA (2009)
7 79 and a cumulative normal distribution one (stochastic) on the basis of a Monte-Carlo simulation (Sgambi et
8 80 al., 2014). The resilience assessment is based on a well-informed resilience index, which is a function of
9 81 the time-variant functionality of the infrastructure over the restoration time for these scenarios. The
10 82 resilience assessment is inclusive of direct and indirect losses for the given seismic scenarios. In this context
11 83 a new cost-based resilience index is also introduced, accounting for the effect of indirect losses in the
12 84 resilience of the assets. The scope of this study is to demonstrate the applicability of the resilience
13 85 assessment framework and to highlight the role of the restoration models, which can be adapted to the
14 86 construction practices that are typically implemented in the region where the bridge is located, the policies
15 87 of the stakeholders, e.g. time required to commence the restoration, and the capabilities of the contractors,
16 88 or the availability of different types of resources, e.g. funds, materials, equipment, human resources. The
17 89 results of this research are expected to facilitate owners to enhance decision-making and risk management
18 90 on the basis of cost-based and well-informed indices toward more resilient infrastructure.
19 91

2. Resilience assessment framework

20 92
21 93 Resilience assessment requires the accurate evaluation of the asset damage for given hazard intensities and
22 94 the realistic simulation of the restoration strategies of the studied system, e.g. transportation network, and
23 95 its assets, e.g. bridges. Resilience is typically correlated with the evolution of asset functionality during the
24 96 recovery process, therefore a time-dependent analysis is enabled in the assessment. Figure 1 illustrates the
25 97 framework that is adopted herein, which encompasses hazard, vulnerability, loss and resilience analysis
26 98 and is applied for representative bridges exposed to earthquakes. In particular, seismic hazard analysis
27 99 defines the hazard Intensity Measures (IM) at the bridge site, based on available hazard models such as the
28 100 2013 European Seismic Hazard Model - ESHM13 (Woessner et al., 2015), which provides seismic hazard
29 101 data on rock conditions. The local site effects on the seismic ground motion can be accounted through
30 102 simplified, yet, rigorous approaches, such as the use of soil amplification factors depending on the soil type
31 103 (Pitilakis et al., 2013).

32 104 The **vulnerability**, which expresses the robustness of the structure, i.e. the ability of the structure to
33 105 withstand seismic loads, is evaluated on the basis of fragility functions for specific typologies of bridges
34 106 (Argyroudis et al., 2019). Fragility functions provide the probability of being or exceeding specific Damage
35 107 States (DS_i) for given IMs, i.e. intact (DS₀), slight damage (DS₁), moderate damage (DS₂), extensive
36 108 damage (DS₃) and failure/collapse (DS₄) as per Equation 1.

$$\text{Fragility} = P[ds > DS_i | IM], i=0, \dots, 4 \quad (1)$$

where P is the probability of damage to exceed a DS_i , $i=0\sim 4$, of the bridge under the excitation of an IM , e.g. PGA.

Direct cost (C_D) due to bridge damage commonly represents the repair costs, evaluated in Equation 2 by multiplying the damage probabilities at various damage states DS_i , with damage ratios (DR) and replacement cost of the bridge (C), according to HAZUS methodology (FEMA, 2009).

$$C_D = C \cdot W \cdot L \sum_{i=0}^4 (P[ds = DS_i | IM] \cdot DR_i) \quad (2)$$

where C is the replacement cost of the bridge per square meter, W and L are the width and the length of the bridge and $P[DS_i | IM]$ is the probability of occurrence of each DS for an event with a given IM :

$P[DS_i | IM] = P[ds > DS_{i+1} | IM] - P[ds > DS_i | IM]$, for $i=1$ to 3 and $P[DS_0 | IM] = P[ds > DS_0 | IM]$ for $i=0$.

The DR quantifies the repair cost as a ratio of the replacement cost of the bridge. FEMA (2009) suggests the following DR for each DS_i : $DR_0=0$, $DR_1=0.03$, $DR_2=0.08$, $DR_3=0.25$ and $DR_4=1$, if $n < 3$ or $= 2/n$, if $n \geq 3$, where n is the number of spans. For example, extensive damage state (DS_3) means that the damage corresponds to a repair cost of about 25% of the replacement cost of the bridge. In some cases, the cost for removal of debris and construction of a temporary bypass is included in the estimation of C_D (Decò et al., 2013).

The **indirect cost (C_{IN})** due to loss of the bridge's functionality, is commonly calculated accounting for the additional costs due to the detour of the traffic. According to Dong & Frangopol (2015) the indirect cost associated with a detour on a bridge can be evaluated as the summation of the operating cost of vehicles on detour (C_{op}) and the cost due to vehicle time loss (C_{TL}) caused by the bridge damage. The C_{op} and C_{TL} can be expressed as in Equation 3 and 4 respectively, modified by the authors to consider a linear reduction of the daily traffic on detour as the repair works of the damaged bridge proceed.

$$C_{op} = \sum_{i=1}^4 \left\{ P[ds = DS_i | IM] \left(T_{id,i} + \frac{1}{2} T_{res,i} \right) \left[C_{op,car} \left(1 - \frac{TR_D}{100} \right) + C_{op,truck} \frac{TR_D}{100} \right] D_i ADT \right\} \quad (3)$$

where $T_{id,i}$ and $T_{res,i}$ are the idle and restoration time, respectively, of a damaged bridge at each DS , $C_{op,car}$ and $C_{op,truck}$ are the average costs of operation of car and truck per kilometer length (\$/km), respectively, D_i is the detour length (km), ADT is the average daily traffic on detour, calculated as 1 minus the average functionality (i.e. weighted with the probabilities of occurrence of each DS) of the examined bridge, multiplied by its average total daily traffic, and TR_D is the average daily truck traffic ratio (%). It is noted that in the present study, Equation 3 was modified by replacing the D_i factor with $D_i - l$, representing the additional route length, where l is the length of the link (km), which would had been traveled by the drivers

1
2
3 146 if the link/bridge was undamaged. This modification was made because, according to the authors,
4
5 147 considering only the additional distance at the calculation of the extra cost seems to be a more rational
6
7 148 approach.

8 149 The cost due to vehicle time loss (C_{TL}) can be estimated based on Equation 4 (Decò et al., 2013, Dong &
9
10 150 Frangopol, 2015).

$$11 151 \\ 12 \\ 13 152 C_{TL} = \sum_{i=1}^4 \left\{ P[ds = DS_i | IM] \left(T_{id,i} + \frac{1}{2} T_{res,i} \right) \left[C_{AW} O_{car} \left(1 - \frac{TR_D}{100} \right) + (C_{ATC} O_{truck} + C_{goods}) \frac{TR_D}{100} \right] \left[ADT \frac{D_i}{S} + ADE \left(\frac{1}{S_D} - \frac{1}{S_0} \right) \right] \right\} \quad (4)$$

14
15 153
16 154 where the terms C_{AW} , C_{ATC} and C_{goods} correspond to the average wage per hour (\$/h), the average total
17 155 compensation per hour (\$/h) and the monetary value of time taken to transport goods in cargo (\$/h),
18
19 156 respectively, O_{car} and O_{truck} are the average vehicle occupancies for car and truck, respectively, S is the
20
21 157 average velocity on detour (km/h), S_D and S_0 are the average velocities (km/h) on the damaged and intact
22 158 bridge, respectively, and ADE is the average daily traffic remaining on the bridge after the seismic event,
23
24 159 calculated by the average functionality of the bridge (i.e. weighted with the probabilities of occurrence of
25 160 each DS) multiplied by its average total daily traffic. Obviously, the summation of ADT and ADE is equal
26
27 161 to the total average traffic.

28
29 162 The **resilience curve** of a bridge subjected to a certain ground shaking level can be generated based on the
30 163 restoration functions, which describe the rapidity of functionality recovery for the different DSs, and the
31
32 164 probabilities of occurrence of each DS.

$$33 165 \\ 34 \\ 35 166 Q(t) = \sum_{i=0}^4 Q[DS_i | t] P[DS_i | IM] \quad (5)$$

36
37 167 where $Q[DS_i | t]$ is the functionality of the bridge being in DS_i , at time t after the commencement of the
38
39 168 restoration, as it is given by the restoration functions.

40
41 169 The **Resilience index** (R) of a bridge can be calculated from the resilience curves and represents the area
42
43 170 under the resilience curve. An efficient way of estimating the resilience index is proposed by Decò et al.,
44
45 171 (2013), as it is shown in Equation 6.

$$46 172 \\ 47 173 \\ 48 174 R = \frac{1}{t_h - t_o} \int_{t_o}^{t_h} Q(t) \quad (6)$$

49
50 175 where t_o is the time of an earthquake occurrence, t_h is the time horizon, such as the time instance where the
51
52 176 bridge has been fully recovered (including the idle and repair time), t is the time variable and $Q(t)$ is the
53
54 177

bridge functionality at time t . The resilience index that accounts for the indirect costs is described in Section 4. The resilience assessment framework of the abovementioned calculation procedure is shown in Figure 1.

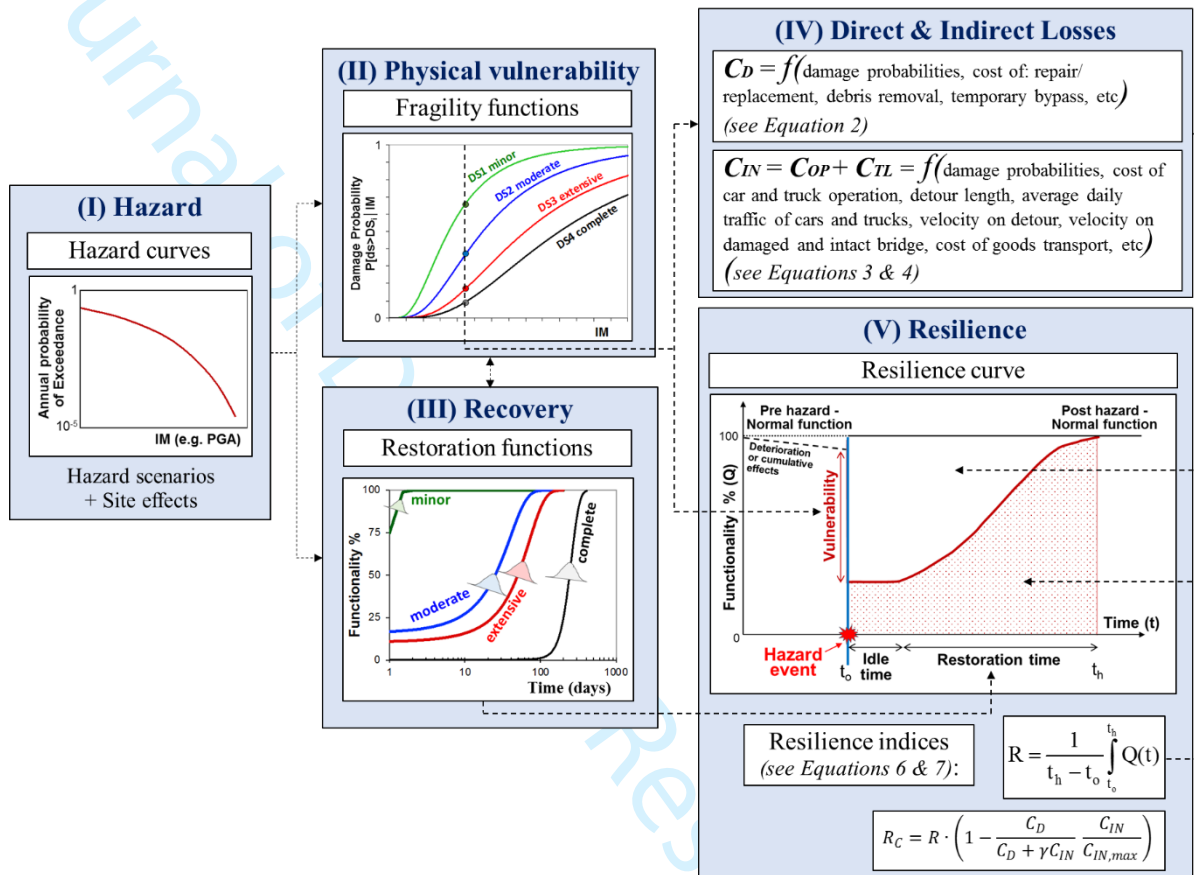


Figure 1. Framework for resilience assessment




3. Application to a portfolio of bridges

3.1 Description of bridges

The three analyzed bridges of this study are given in Table 1. The bridges are classified according to Moschonas et al., (2009) based on three critical typology parameters, which are: (1) type of piers, (2) type of deck and (3) type(s) of pier-to-deck connections. In the following, these three bridges are named after “Bridge 1”, “Bridge 2” and “Bridge 3”. Bridge 1 is located at Neapoli’s Valley and it was built in 1984. It is a three-span bridge of total length 120 m, having simply-supported precast and prestressed beams connected through a continuous reinforced concrete slab that is supported through bearings on multicolumn bents with surface foundations. Bridge 2 is located at interchange K12 along the Ring Road and it was built in 1992. It has three-spans and a total length of 77 m, having a cast-in-situ box-girder (triple cell) deck supported through bearings on wall-type piers with pile foundations. Bridge 3 is located at interchange K8 and was constructed in 2002. It is a seven-span bridge with a total length of 147 m and has a box-girder (single-cell) deck, which is either rigidly connected to the single-column hollow rectangular piers or seating upon them through bearings. The piers are founded on superficial foundations. For all the bridges described above the abutments are typical seat-type abutments with expansion joints and bearings. Thus, Bridge 1,

Bridge 2 and Bridge 3 correspond to types 332, 422 and 223, respectively, according to the Moschonas et al., (2009) classification. Bridges 1 and 3 are located on a rock formation (ground type A), while Bridge 2 is founded on very dense sand to clay soil formation (ground type B2, according to the classification proposed by Pitilakis et al., 2013).

Table 1. Portfolio of bridges along the ring-road of Thessaloniki

Bridge	Location	Construction Method	Construction Year	Spans	Length/ Width (m)	Foundation Type
 1	Neapoli's Valley	Precast I-beams with continuous deck slab	1984	3	120/ 22	Shallow
 2	Interchange K12	Cast in-situ box girder deck	1992	3	77/ 14	Piles
 3	Interchange K8	Cast in-situ box girder deck	2002	7	147/ 11	Shallow

3.2 Seismic hazard

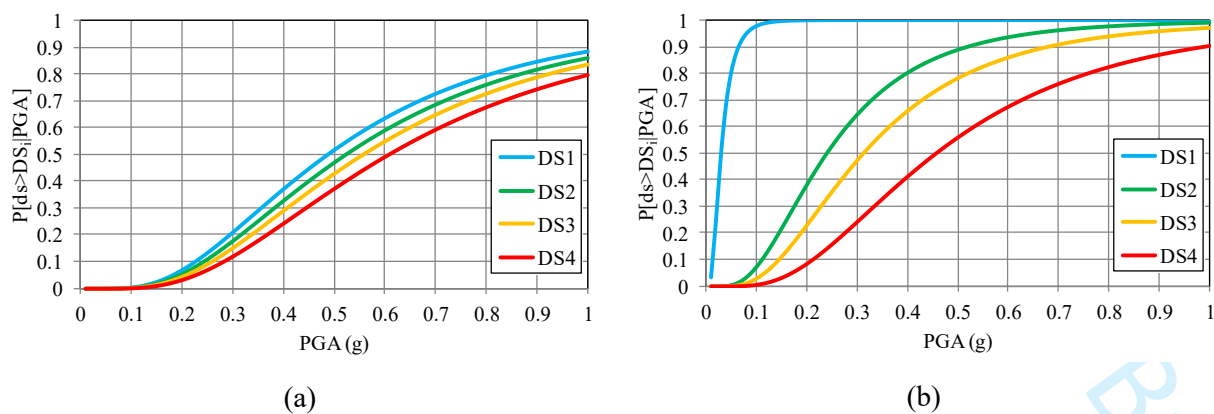
The three bridges of this case study are analyzed for two seismic scenarios. The first one refers to an earthquake with a probability of exceedance equal to 10% in 50 years (Scenario I) corresponding to a return period of 475 years and the second with probability 5% in 50 years (Scenario II) corresponding to a return period of 975 years. The intensity measure that has been chosen is the PGA, which is obtained on rock conditions for each bridge location, using the hazard curves provided by the ESHM13 (Woessner et al., 2015). To account for the local soil conditions the obtained PGA_{rock} values are multiplied by an amplification soil factor, S_{soil} , (Pitilakis et al, 2013, for $M_s > 5.5$). The estimated PGA values are shown in Table 2 and they are used to calculate the exceedance and occurrence probabilities of specific DS based on the selected fragility curves.

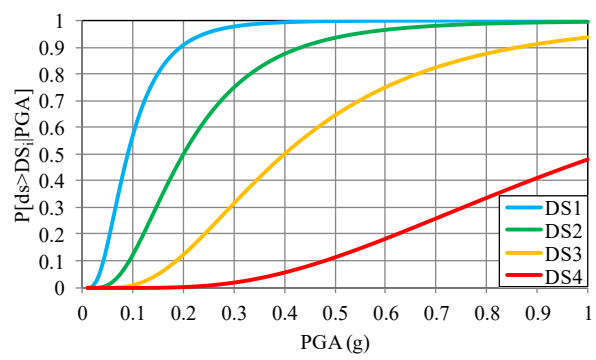
Table 2. PGA values at the site of the three bridges

Bridge	S_{soil}	Scenario	PGA_{rock} (g)	PGA (g)
1	1.0	I	0.26	0.26
		II	0.38	0.38
2	1.3	I	0.26	0.34
		II	0.38	0.49
3	1.0	I	0.28	0.28
		II	0.40	0.40

3.3 Vulnerability analysis

The fragility functions used for the vulnerability assessment are based on the study of Moschonas et al., (2009) for bridges constructed with the latest seismic provisions, i.e. after 1993. The fragility functions were developed based on numerical modelling, using damage criteria defined by the yielding and the ultimate displacements of the bridge and the abutment-backfill system as well as the expansion joint width (gap). For the needs of this study, the response of the bridge in the longitudinal direction is considered only, taking into account the abutment-backfill interaction including gap closure. It is also recognized that bridges designed without advanced provisions exhibit greater vulnerabilities than the once designed based on guidelines on earthquake resistance. Due to the absence of available and compatible fragility functions, for taking into account the reduced capacity of bridges designed prior to 1993, a factor, S_{year} , is introduced that increases the median threshold values of the intensity measure (PGA_{im}) required for causing the DS_i . This factor was chosen based on expert judgment and was reflected by reducing the capacity per decade of construction prior to 1993, as follows: 2.5% for DS1, 5% for DS2, 7.5% for DS3 and 10% for DS4. The reduction was considered as different at each DS, because a bridge constructed before 1993 is expected to be less resilient for larger-scale damages. As an exception, for Bridge 2, which was constructed in 1992, S_{year} was chosen equal to 1.0 for DS1 and DS2, 0.025 for DS3 and 0.05 for DS4. For Bridge 3, the median values were unchanged and equal to 0.09 for DS1, 0.20 for DS2, 0.32 for DS3 and 0.48 for DS4. The modified fragility parameters are shown in Table 3 and the fragility curves, which follow a lognormal cumulative distribution function, are illustrated in Figure 2. It is noted that the total lognormal standard deviation is constant for all DSs and was not modified, i.e. $\beta_{tot}=0.6$. The calculated damage probabilities for the two seismic scenarios are shown in Table 4.





(c)

Figure 2. Fragility curves for PGA at the soil surface for: (a) Bridge 1, (b) Bridge 2 and (c) Bridge 3

Table 3. Fragility parameters for the Bridges 1 and 2

Bridge	Construction year	DS	S_{year}	$PGA_{im} (g)$	$PGA_{im} (reduced) (g)$
1	1984	1	0.976	0.50	0.49
		2	0.952	0.55	0.52
		3	0.930	0.60	0.56
		4	0.909	0.67	0.61
2	1992	1	1.000	0.03	0.03
		2	1.000	0.24	0.24
		3	0.976	0.32	0.31
		4	0.952	0.48	0.46

Table 4. Probabilities of exceedance and occurrence of each DS for the three bridges subject to two seismic scenarios

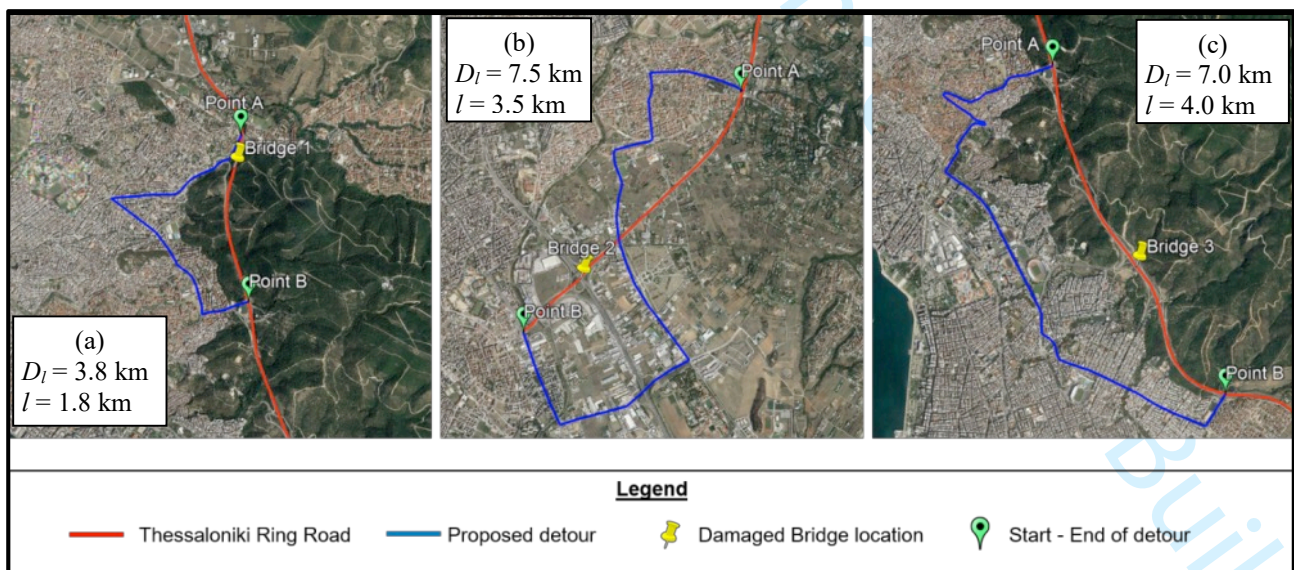
Bridge 1				
	Seismic Scenario I		Seismic Scenario II	
DS	P[ds>DS_i PGA]	P[DS_i PGA]	P[ds>DS_i PGA]	P[DS_i PGA]
0	1.00	0.85	1.00	0.66
1	0.15	0.03	0.34	0.04
2	0.12	0.02	0.30	0.04
3	0.10	0.02	0.26	0.04
4	0.08	0.08	0.22	0.22
Bridge 2				
	Seismic Scenario I		Seismic Scenario II	
DS	P[ds>DS_i PGA]	P[DS_i PGA]	P[ds>DS_i PGA]	P[DS_i PGA]
0	1.00	0.01	1.00	0.01
1	0.99	0.27	0.99	0.11
2	0.72	0.16	0.88	0.11
3	0.56	0.25	0.77	0.23
4	0.31	0.31	0.55	0.55
Bridge 3				
	Seismic Scenario I		Seismic Scenario II	
DS	P[ds>DS_i PGA]	P[DS_i PGA]	P[ds>DS_i PGA]	P[DS_i PGA]
0	1.00	0.03	1.00	0.01
1	0.97	0.26	0.99	0.12
2	0.71	0.44	0.88	0.38
3	0.28	0.26	0.50	0.44
4	0.02	0.02	0.06	0.06

3.4 Direct and indirect costs

The direct costs (C_D) of the examined bridges are evaluated according to Equation 2 and the probabilities of Table 4, using typical construction costs of bridges in Greece. These costs depend mainly on the construction method and their complexity and they were estimated as $C_1=1500$ \$/m² for Bridge 1, $C_2=1800$ \$/m² for Bridge 2 and $C_3=2000$ \$/m² for Bridge 3. The DRs of each DS have been considered as $DR_0=0$, $DR_1=0.03$, $DR_2=0.08$, $DR_3=0.25$ and $DR_4=0.75$. $DR_0 \sim DR_3$ as per Werner et al., (2006), while DR_4 has been modified by the authors to 0.75, in order to represent the multi-span bridge failure or collapse conditions.

For the estimation of the indirect losses (C_{IN}) due to traffic deviations, an alternative detour is proposed for each one of the examined bridges, as shown in Figure 3. The indirect cost is estimated based on Equations 3 and 4, and the values of the relevant parameters were defined based on available data, expert judgment and evidence in available literature (Venkittaraman & Banerjee, 2014). In particular, $C_{op,car}$ was considered

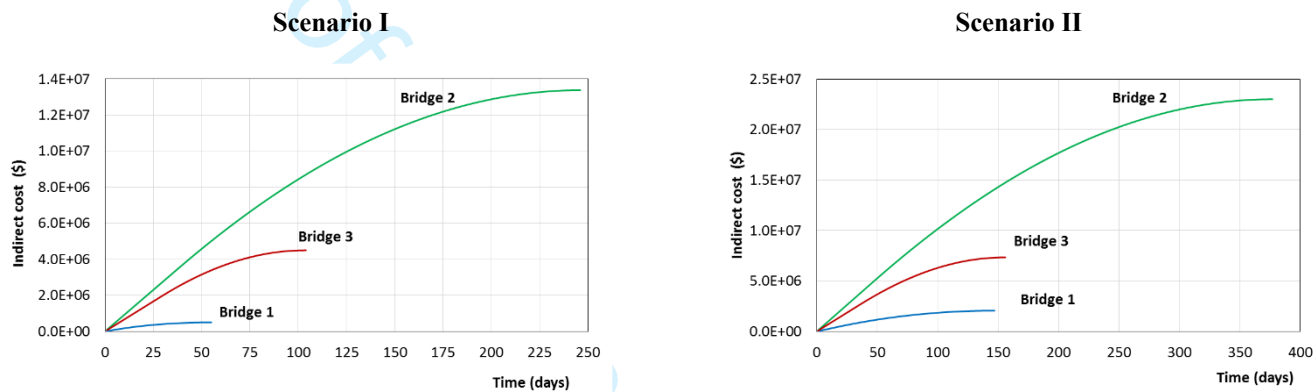
1
 2
 3 260 equal to 0.20 and $C_{op, truck}$ equal to 0.30 \$/km, $TR_D = 20\%$, both C_{AW} and C_{ATC} were taken equal to 7 \$/h, O_{car}
 4
 5 261 $= 2.0$ and $O_{truck} = 2.0$, $C_{goods} = 3$ \$/h, $S_D = 50$ km/h, $S_0 = 90$ km/h and $S = 40$ km/h. The ADE and ADT were
 6
 7 262 considered as fractions of the average daily traffic, which was set equal to 50,000 vehicles per day based
 8
 9 263 on the local traffic conditions. Specifically, ADE was considered equal to the remained functionality of the
 10
 11 264 bridge at each DS multiplied by the average daily traffic (i.e. 50,000 vehicles per day), while ADT is equal
 12
 13 265 to the difference between the average daily traffic and the ADE at each DS. The post-event functionality at
 14
 15 266 each DS was defined as 75% for DS1, 25% for DS2, 10% for DS3 and 0% for DS4, as per FEMA (2009).
 16
 17 267 The low functionality in extensive damage corresponds to emergency mobility. It is noted that the
 18
 19 268 functionality of a bridge at each DS is considered as the percentage of the bridge capacity to sustain loads
 20
 21 269 and is proportional to the ability of the bridge to carry traffic. This means that a bridge with functionality
 22
 23 270 equal to 50% can bear only half of the normal traffic loads. However, this is an assumption that might be
 24
 25 271 adapted according to case-specific conditions and requirements of the stakeholders or contractors, for
 26
 27 272 example, traffic can be completely prohibited until bridge repair is completed.
 28
 29 273 The estimated costs (direct, indirect, and total) for the three bridges are shown in Table 5 for the two
 30
 31 274 earthquake scenarios. The indirect losses' increment as a function of time is shown in Figure 4. It is
 32
 33 275 observed that the higher the seismic intensity the higher the repair costs, because the IMs, and hence the
 34
 35 276 damage probabilities, are higher. Although Bridge 3 has the largest area and repair cost per square meter
 36
 37 277 from the three bridges examined, the highest costs are estimated for Bridge 2 for both scenarios. This is due
 38
 39 278 to the higher vulnerability of Bridge 2 and the relatively long detour length. Also, Bridge 2, has the highest
 40
 41 279 C_D/C_{IN} ratio, as the indirect losses are expected to be about 25 times more than the direct losses for Scenario
 42
 43 280 II. The lowest C_D/C_{IN} ratio was estimated for Bridge 1, i.e. about 4 for both scenarios. The estimated ratios
 44
 45 281 are in good agreement with past studies on highway bridges, which have considered the indirect losses 5 to
 46
 47 282 20 times greater than the direct losses (Venkittaraman & Banerjee 2014).



48
 49
 50
 51
 52
 53
 54
 55
 56 283
 57
 58 284 **Figure 3.** Alternative detours for (a) Bridge 1, (b) Bridge 2 and (c) Bridge 3. D_l is the detour length (blue
 59 285 line) and l is the length of the link (distance from point A to B on the red line).

Table 5. Direct (repair) and indirect costs of the Thessaloniki's Ring Road examined bridges

Bridge	Scenario I				Scenario II			
	Direct (C_D)	Indirect (C_{IN})	Total (C_{TOT})	Ratio (C_{IN}/C_D)	Direct (C_D)	Indirect (C_{IN})	Total (C_{TOT})	Ratio (C_{IN}/C_D)
1	\$ 264,651	\$ 545,416	\$ 810,067	2.1	\$ 702,279	\$ 2,116,326	\$ 2,818,605	3.0
2	\$ 612,670	\$ 13,137,513	\$ 13,750,183	21.4	\$ 928,214	\$ 22,368,967	\$ 23,297,181	24.1
3	\$ 385,525	\$ 4,444,235	\$ 4,829,760	11.5	\$ 606,013	\$ 7,145,407	\$ 7,751,420	11.8

**Figure 4.** Cumulative indirect loss for the three bridges and the two seismic scenarios

3.5 Resilience analysis

The repair time for each DS and bridge has been estimated by selecting realistic repair works from Karamlou & Bocchini (2017), as it is shown in Table 6. The selection was made on the basis of the bridge characteristics typology and geometry and the definition of the DSs. The duration of the repair tasks in the present application was adjusted based on engineering judgement considering realistic local construction practices. For example, the increased time for realignment or replacement of bearings in Bridge 1, is due to the large number of bearings and the limited access to the pier caps due to the height of the bridge. Additionally, no damage is expected on the piers of Bridge 1 as they are fully isolated with bearings, whereas in Bridge 3 there are piers rigidly connected to the deck and hence damage is expected. Furthermore, it is assumed that the repair tasks are subsequent, i.e. in series. Since the duration of the repair tasks is described by Karamlou & Bocchini (2017) using a triangular or uniform probability distribution, as far as the deterministic approach is concerned, the total restoration times for DS1 to DS3 were obtained by adding the mode value of each triangular distribution and the upper values of each uniform distribution. For the stochastic analysis, and also for the deterministic analysis for DS4, a Monte Carlo simulation (10^5 samples) was employed to probabilistically model the restoration time of the repair works, using a normal distribution (Table 6).

Table 6. Repair works and their duration for the three bridges

DS	Task ID	Task description	Distribution	Bridge 1	Bridge 2	Bridge 3
				Lower/ Mode/Upper		
DS1	1.1	Repair minor spall	Triangular	2 / 4 / 6	2 / 4 / 6	2 / 4 / 6
	1.2	Repair cracks with epoxy	Triangular	4 / 7 / 11	4 / 7 / 11	4 / 7 / 11
	1.3	Realign the bearings	Uniform	5 / - / 10	1 / - / 5	3 / - / 8
	Total mean restoration time			21	16	19
DS2	2.1	Repair moderate spall	Triangular	3 / 6 / 9	3 / 6 / 9	3 / 6 / 9
	2.2	Repair cracks with epoxy	Triangular	4 / 8 / 12	4 / 8 / 12	4 / 8 / 12
	2.3	Realign bearings	Uniform	5 / - / 10	1 / - / 5	3 / - / 7
	2.4	Replace expansion joint	Triangular	4 / 7 / 10	4 / 7 / 10	4 / 6 / 8
	2.5	Repair continuous slabs	Triangular	1 / 2 / 4	-	-
	2.6	Repair of backwalls	Triangular	2 / 10 / 20	2 / 10 / 20	6 / 12 / 18
	2.7	Repair box girder cracks	Triangular	-	5 / 10 / 15	5 / 10 / 15
	2.8	Repair piers	Triangular	-	-	5 / 10 / 15
Total mean restoration time			43	46	59	
DS3	3.1	Repair extensive spall	Triangular	4 / 8 / 12	4 / 8 / 12	4 / 8 / 12
	3.2	Repair cracks with epoxy	Triangular	4 / 8 / 12	4 / 8 / 12	4 / 8 / 12
	3.3	Remove/construct new bearing pedestals	Triangular	1 / 2 / 3	1 / 2 / 3	1 / 2 / 3
	3.4	Install new bearings	Uniform	10 / - / 20	4 / - / 8	5 / - / 10
	3.5	Replace expansion joint	Triangular	4 / 7 / 10	4 / 7 / 10	4 / 6 / 8
	3.6	Reconstruct continuous slabs	Triangular	4 / 6 / 8	-	-
	3.7	Repair abutments (backwall, backfill, approach slabs, wing walls)	Triangular	9 / 18 / 30	9 / 18 / 30	9 / 18 / 30
	3.8	Repair bent caps	Triangular	10 / 20 / 30	-	-
	3.9	Repair piers	Triangular	-	5 / 10 / 15	15 / 30 / 45
	3.10	Repair box girder	Triangular	-	9 / 18 / 30	9 / 18 / 30
	3.11	Repair foundation	Triangular	15 / 30 / 45	15 / 30 / 45	15 / 30 / 45
Total mean restoration time			119	109	130	
DS4	4.1	Reconstruction of bridge	Normal	$\mu = 1080$ $\sigma = 216$	$\mu = 720$ $\sigma = 144$	$\mu = 1080$ $\sigma = 216$

Apart from the repair time shown in Table 6, an idle time at each DS was also considered based on engineering judgement, equal to 15 days for DS1, 30 days for DS2, 45 days for DS3 and 60 days for DS4. The increasing idle time was considered to be a rational approach as worse DS would require more time

for the owner to react and commence restoration works. The post-event functionality at each DS was assumed to be 75% for DS1, 25% for DS2, 10% for DS3 and 0% for DS4, as per FEMA (2009) as discussed in the previous section. In Figure 6, both the linear deterministic and the Monte Carlo stochastic restoration curves of the examined bridges are presented. For the Monte Carlo simulation, a cumulative normal distribution was assumed. The mean, μ , and standard deviation, σ , used for each DS of each bridge (Table 7) were calculated based on a statistic process as it is shown in Figure 5. It is noted that μ at DS4 was assumed as five times larger than μ at DS3, as well as σ at DS4 was assumed equal to 35% of μ at the same DS.

In addition to the restoration curves at each DS, also the resilience curves are plotted for the two scenarios as per Equation 5. For the deterministic analysis, these curves are plotted considering the post-event functionality, the idle and the repair time, weighted with the probability of occurrence of each DS. In the stochastic analysis, the resilience curves are based on the consideration of μ and σ , weighted with the probability of occurrence of each DS.

Table 7. Mean and standard deviation of restoration time normal distribution at each DS for the three examined bridges

DS	Bridge 1 (days)	Bridge 2 (days)	Bridge 3 (days)
1	$\mu = 18.8$	$\mu = 14.3$	$\mu = 16.8$
	$\sigma = 2.2$	$\sigma = 2.0$	$\sigma = 2.2$
2	$\mu = 41.5$	$\mu = 44.7$	$\mu = 57$
	$\sigma = 4.7$	$\sigma = 5.0$	$\sigma = 4.5$
3	$\mu = 114$	$\mu = 109$	$\mu = 129.5$
	$\sigma = 9.2$	$\sigma = 9.3$	$\sigma = 11$
4	$\mu = 570$	$\mu = 545$	$\mu = 647.5$
	$\sigma = 199.5$	$\sigma = 190.8$	$\sigma = 226.6$

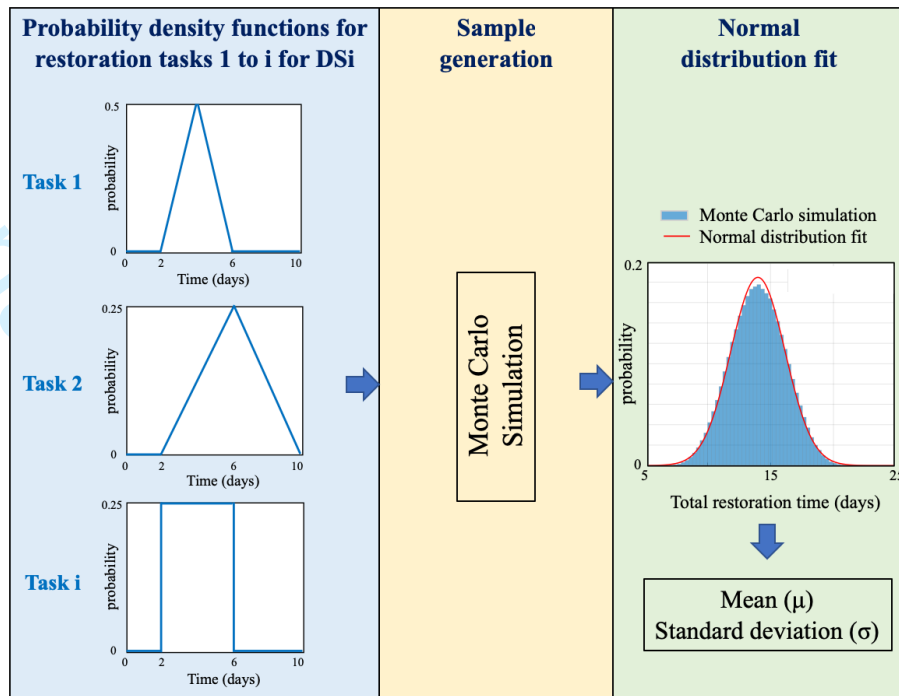


Figure 5. Statistic process for the estimation of the mean (μ) and standard deviation (σ) of the restoration time after a specific damage state.

Due to the fact that the idle time was the same for the three bridges and the restoration time was similar for each DS of the three examined bridges, the restoration diagrams for the two approaches (left and right column in Figure 7) are almost alike. However, the resilience curves (black dashed lines in Figure 6) are different for each bridge, as these are strongly dependent on the probability of occurrence of each DS. The Resilience indices were calculated based on Equation 6, and normalized with respect to the DS4 total restoration time of each bridge as it is shown in Table 8. It is noted that the DS4 restoration time as resulted by the Monte Carlo analysis is significantly longer than the corresponding one for the deterministic analysis. This is due to the fact that the deterministic linear approach is based merely on the mean value of the estimated duration of each restoration task, while on the other hand, the stochastic Monte Carlo approach takes into account the probability density function of each task. Therefore, Monte Carlo approach depends also on the cumulative function of the fitted to the restoration tasks normal distribution, as Figure 5 implies. For both the stochastic and deterministic approaches, it is observed that the Resilience index gradually reduces as the DS shifts from 1 to 4. Moreover, since the restoration time is similar for each DS for the three bridges examined, the Resilience indices are also similar for each DS. For both approaches, R values are similar in the case of DS1 to DS3, with slightly larger values observed in the stochastic approach. In the case of DS4, a dispersion of R values is observed between the two approaches (stochastic analysis having smaller values than the deterministic one). This is due to the fact that, as it has been already mentioned, Monte Carlo assigns significantly longer total restoration time. Hence, for this particular case study, the resilience is almost independent of the type of model of the restoration time (linear, stochastic) for DS1~DS3, while somehow worth mentioned deviations are observed in the case of DS4.

The R values obtained by the resilience curves for the two scenarios vary between the three bridges as the damage probabilities affect the estimation of resilience indices. However, the deterministic and stochastic approaches give similar estimations. Overall, Bridge 1 has the highest resilience index due to lower vulnerability, while R values, as expected, are lower for the more severe scenario (II). The variation of R values with the examined total restoration time for the four DSs is shown in Figure 7, where the difference between the two approaches is significant for DS4, again because of the longer restoration time that Monte Carlo analysis assigns. It is noted that the diagrams in Figure 7 should be read as functions that give different R values for different total restoration time and asymptotically approach the full functionality equal to 100%. Therefore, for the cases examined in the present study, the R values correspond to the examined bridges' total restoration time should be taken into account, i.e. for all cases, the R values were calculated considering the same final time (t_f) for both the linear and the Monte-Carlo models. The final time t_f (i.e. time horizon) was considered equal to 1200 days, which is approximately 3 years. Observing Figure 7, it is noted that there is a significant discrepancy between the R values of DS4 for linear deterministic and stochastic Monte Carlo analysis. This is attributed to the fact that the first approach has a fixed value for the duration of the restoration tasks, whereas the stochastic simulation has large standard deviations, which are of increasing value for more severe DSs, e.g. DS4.

Table 8. Resilience indices (R) of the examined bridges for each DS and seismic scenario, based on deterministic and stochastic analysis

R	Bridge 1		Bridge 2		Bridge 3	
	Deterministic	Stochastic	Deterministic	Stochastic	Deterministic	Stochastic
1	0.995	0.993	0.995	0.994	0.995	0.993
2	0.968	0.964	0.967	0.963	0.963	0.955
3	0.922	0.903	0.925	0.907	0.918	0.892
4	0.713	0.512	0.723	0.533	0.680	0.448
Scenario I	0.997	0.994	0.914	0.852	0.964	0.946
Scenario II	0.980	0.964	0.848	0.730	0.939	0.901

1
2
3
4
5
6
7
8
9
10
11
12
13
14
15
16
17
18
19
20
21
22
23
24
25
26
27
28
29
30
31
32
33
34
35
36
37
38
39
40
41
42
43
44
45
46
47
48
49
50
51
52
53
54
55
56
57
58
59
60

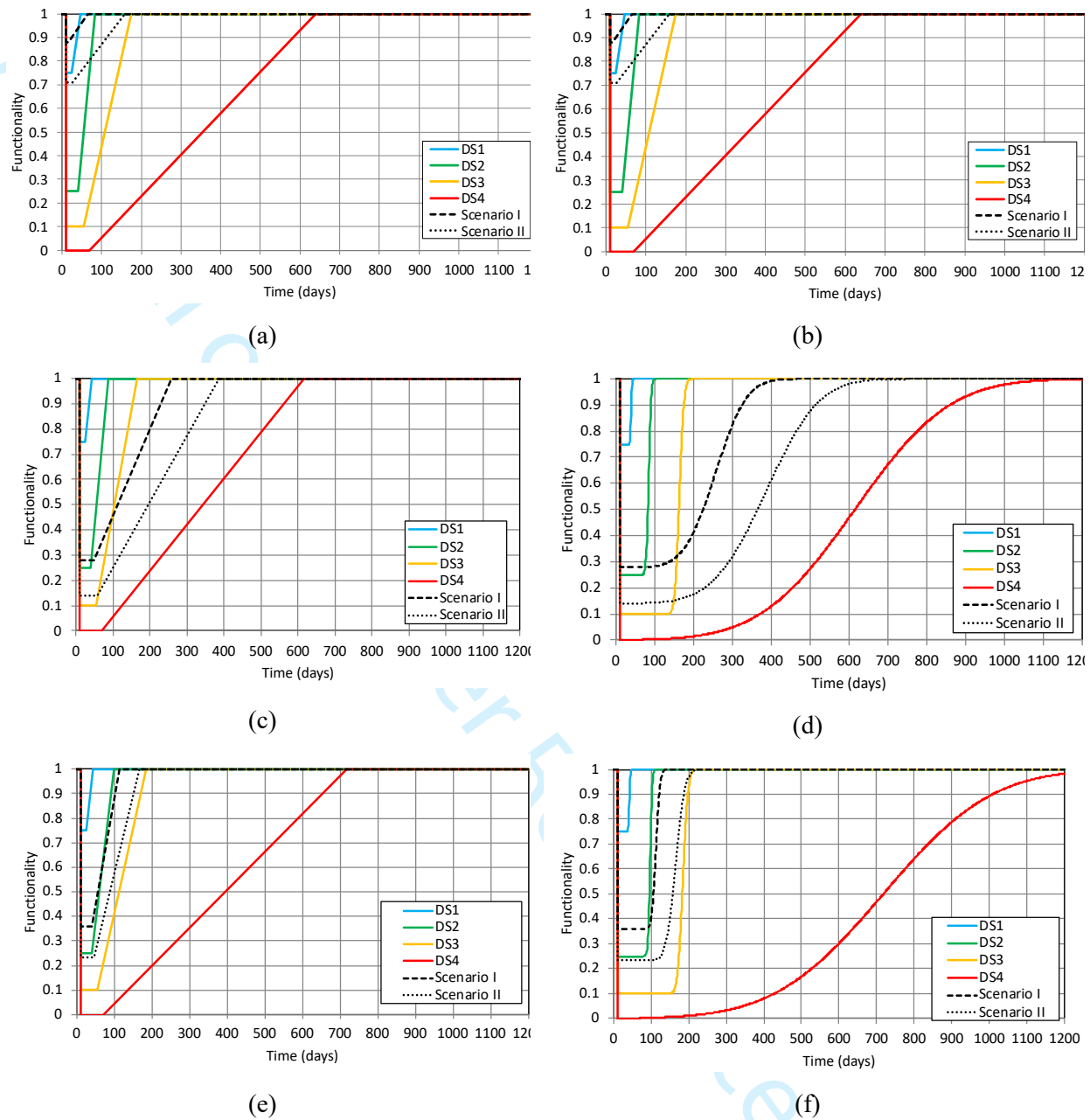


Figure 6. Deterministic linear (left column) and stochastic Monte Carlo (right column) restoration and resilience curves for: (a-b) Bridge 1, (c-d) Bridge 2 and (e-f) Bridge 3

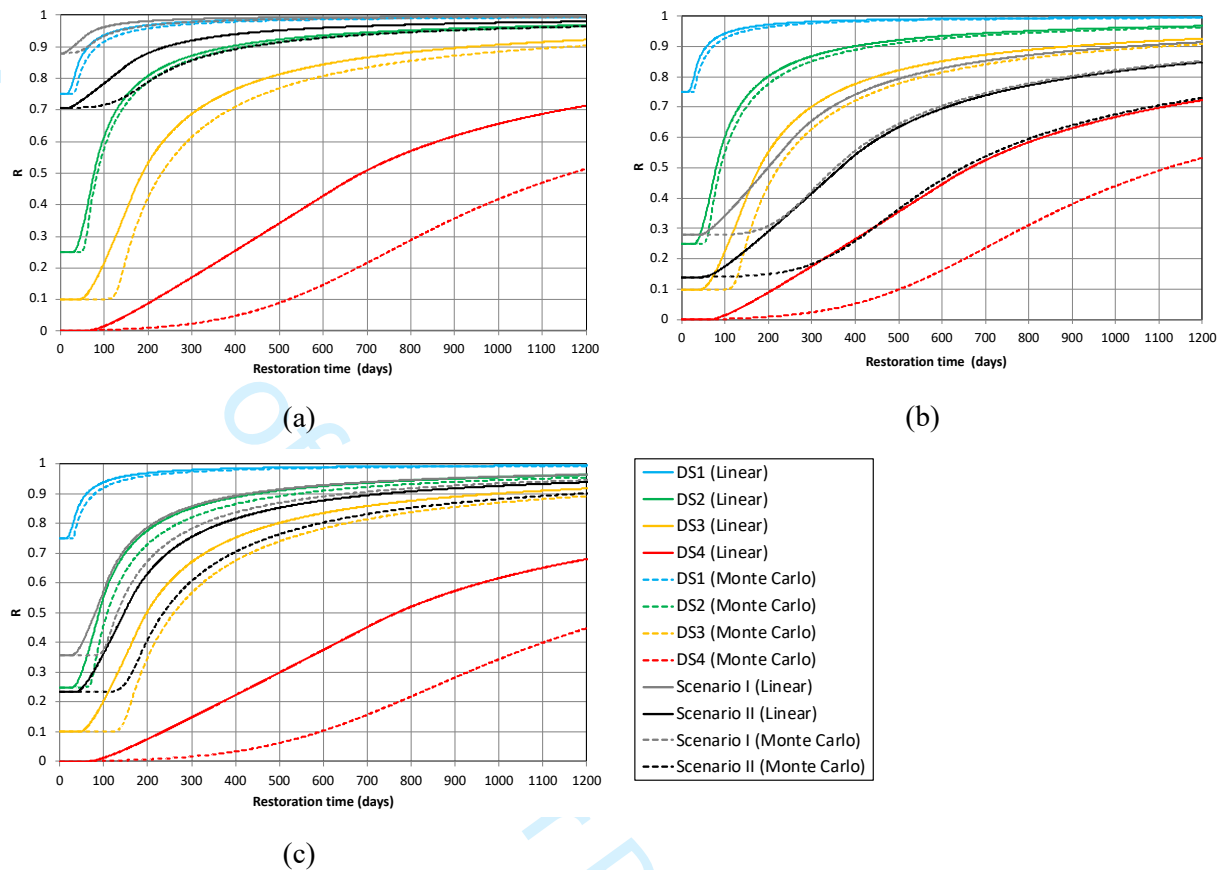


Figure 7. Temporal variation of resilience ratios for: (a) Bridge 1, (b) Bridge 2 and (c) Bridge 3 for linear deterministic and stochastic Monte Carlo analysis

4. Cost-based resilience index

The loss of resilience is a measure of the lost functionality (Q), which can be measured by the resilience of the perfectly resilient asset, $R=1$, minus the resilience index as calculated by Equation 6, which is smaller than 1, due to the occurrence of the seismic events. However, the loss of functionality of a bridge might be related to structural (direct) losses or other obstructions, e.g. debris on the bridge due to an earthquake-triggered landslide, the latter not necessarily inducing any structural damage (direct losses). The loss of functionality of the bridge will also result in indirect losses, which are consequences of the loss of resilience ($1-R$), such as the losses due to detour of traffic or business interruption. As the loss in resilience is not a measure of the direct and indirect monetary losses, a new resilience index is introduced, R_C , which encapsulates socio-economic consequences (direct and indirect losses) in the resilience assessment. This paper only included three bridges as the critical assets of the transport network, and hence the R_C is normalised with respect to the bridge that has the greatest indirect loss in the portfolio. A similar concept is also applicable for assessing the resilience of portfolios of transport assets within a network and interdependent networks.

In particular, a cost-based resilience index, R_C , is defined in Equation 7, which is essentially an adjustment of the streamlined resilience index R , given in Equation 6, accounting for the direct and indirect losses.

$$R_C = R \cdot \left(1 - \frac{C_D}{C_D + \gamma C_{IN}} \frac{C_{IN}}{C_{IN,max}} \right) \quad (7)$$

where, C_D and C_{IN} correspond to the direct and indirect cost of the bridge and γ is a factor that takes into account the socio-economic impact of the indirect cost on the network operation compared to the direct losses. The value of γ is chosen by the stakeholders based on expert judgement, considering the socio-economic impact of a bridge failure on the transportation infrastructure, on the basis of damage extent, daily traffic, or accessibility to critical facilities (Cimellaro, 2016). According to the authors, a rational range of γ is between 0.05 and 0.15 (in the present study γ was set equal to 0.15). $C_{IN,max}$ is the maximum indirect cost estimated for the portfolio of bridges under study. Obviously, for a single bridge or for the bridge having the maximum indirect cost within the portfolio, C_{IN} coincides with $C_{IN,max}$ and, hence, the ratio of C_{IN} to $C_{IN,max}$ is equal to one.

Therefore, R_C is the streamlined R index decreased by two factors. The first one is related to the socio-economic importance of the indirect loss of the examined bridge compared to its direct one, while the second factor normalizes this indirect cost of the bridge in accordance with the maximum indirect cost of the examined portfolio. The R_C values calculated in the present study are compared with the R values in Table 9, for the two seismic scenarios. It is observed that the higher impact of the indirect losses is estimated in the resilience of Bridge 2. This is also defined by the ratio of R_C to R, which describes the importance of the indirect costs in the resilience of each asset, i.e. the lower the ratio the most critical is the asset in terms of indirect losses. In this context, R_C may be utilized as an additional decision-making tool, reflecting the consequences of indirect losses for different hazard scenarios, providing an objective means to facilitate decision-making by the stakeholders and network operators for efficient allocation of resources.

Table 9. Cost-based resilience indices (R_C) for the examined portfolio of bridges

Bridge	Scenario I			Scenario II		
	R	R_C	R_C/R	R	R_C	R_C/R
1	0.997	0.965	0.968	0.980	0.916	0.935
2	0.914	0.697	0.763	0.848	0.664	0.783
3	0.964	0.939	0.974	0.939	0.831	0.885

5. Conclusions

This paper studied the resilience of three representative road bridges on the basis of a framework that encompasses hazard, vulnerability and restoration analysis. The resilience was evaluated, in terms of direct and indirect losses and restoration times for two seismic scenarios. The duration of the repair tasks was adjusted considering realistic local construction practices. The new evidence that this paper provides is the evaluation of resilience based on two commonly accepted, but different approaches for the modelling of

the restoration tasks. These approaches are a simplified deterministic linear model in which the post-disaster functionality, i.e. during the restoration process, is a linear equation of the time and a stochastic one, where the uncertainty is addressed with streamlined statistics methods. The results are compared in terms of the resulting resilience indexes. This study came up with the following conclusions.

There are differences between the two approaches with the stochastic one believed to be the most accurate one. The differences are minor for less critical damage states, whereas appear to be significant for the complete damage scenarios. This is attributed to the standard deviation considered in the stochastic approach, which is higher in more severe damage states, e.g. DS4. This means that linear models are adequately accurate for less severe damage states, e.g. DS1, DS2, DS3, which makes them appropriate for managing minor to moderate post-hazard damage. Systematically the linear model is less conservative than the Monte-Carlo approach as it overestimates the resilience index, R . Regarding the R values for different bridge types and locations, the curved in-plane bridge (Bridge 3) has the lowest resilience. This is reflected both by the vulnerability of the structure, which leads to higher loss of functionality, and time-consuming restoration actions also related to the difficulty in accessing the bridge, because this is an overpass of the busy ring road of the city, which makes any restoration tasks more challenging. The other two bridges have similar resilience. In regard to the impact of indirect losses to the resilience of the three bridges, Bridge 2 is most critical, followed by Bridge 1 and Bridge 3. This is due to the higher vulnerability of Bridge 2 and the longer detour length for this particular bridge.

The value of the proposed framework and application at the asset level is the encapsulation of the direct and indirect losses and recovery process in two indices, which can facilitate the efficient allocation of resources, planning and interventions by the owners, toward safer and more resilient transport infrastructure. Thus, it is essential for the owners to define, with the help of engineers, appropriate thresholds for the resilience indices to expedite the decision-making according to their needs and priorities. The proposed framework and indices is of particular interest for, but not limited to, controlled access motorways such as a ring road of a city or a high-speed road, where there are not many alternative routes. The application at a wider network scale should also incorporate other factors toward a well-informed resilience-based decision making, on the basis of network analysis, including post-earthquake traffic demand variation as well as economic, social and environmental consequences, due to physical damage and traffic diversions.

References

- Almufti, I., & Willford, M.R. (2013). Resilience-based Earthquake Design (REDi) Rating System, version 1.0. Arup. 4
- Akiyama, M., Frangopol, D. M., Ishibashi, H. (2019). Toward life-cycle reliability-, risk-and resilience-based design and assessment of bridges and bridge networks under independent and interacting hazards: emphasis on earthquake, tsunami and corrosion. *Structure and Infrastructure Engineering*, [https://doi:10.1080/15732479.2019.1604770](https://doi.org/10.1080/15732479.2019.1604770).

- 1
2
3 467 Ayyub, B.M., (2014). Systems resilience for multihazard environments: Definition, metrics, and valuation
4 for decision making. *Risk Analysis*, 34(2), 340-355.
- 6 469 Argyroudis, S.A., Mitoulis, S.A., Hofer, L., Zanini, M.A., Tubaldi, E., Frangopol, D.M. (2020). Resilience
8 470 assessment framework for critical infrastructure in a multi-hazard environment. *Science of the Total*
9 471 *Environment*, 714, 136854.
- 11 472 Argyroudis, S., Mitoulis, S.A., Winter, M.G., & Kaynia, A.M. (2019). Fragility of transport assets exposed
12 to multiple hazards: State-of-the-art review toward infrastructural resilience. *Reliability Engineering*
13 473 *and System Safety*, 191, 106567.
- 16 475 Banerjee, S., Vishwanath, B. S., & Devendiran, D. K. (2019). Multihazard resilience of highway bridges
17 476 and bridge networks: a review. *Structure and Infrastructure Engineering*, 15(12), 1694-1714.
- 19 477 Basoz, N., Kiremidjian, A., King, S., & Law, K. (1999). Statistical analysis of bridge damage data from the
20 478 1994 Northridge, CA, Earthquake. *Earthquake Spectra* , 15 (1), 25-54.
- 22 479 Billah, A., & Alam, M. (2015). Seismic fragility assessment of highway bridges: a state-of-the-art- review.
23 *Structure and Infrastrure Engineering* , 11 (6), 804-832.
- 25 481 Bocchini, P., & Frangopol, D. (2012a). Optimal resilience and cost based post-disaster intervention
26 482 prioritization for bridges along a highway segment. *Journal of Bridge Engineering* , 17 (1), 117-129.
- 28 483 Bocchini, P., & Frangopol, D.M. (2012b). Restoration of bridge networks after an earthquake: multi-criteria
29 484 intervention optimization. *Earthquake Spectra*, 28(2), 427-455.
- 31 485 Bocchini, P., Decò, A., & Frangopol, D. (2012). Probabilistic functionality recovery model for resilience
32 486 analysis. In F. Biondini, & D. Frangopol (Ed.), *Bridge Maintenance, Safety, Management, Resilience*
33 487 *and Sustainability*. London. Taylor & Francis Group.
- 36 488 Bruneau, M., Chang, S.E., Eguchi, R.T., Lee, G.C., O'Rourke, T.D., Reinhorn, A.M., Shinozuka, M.,
37 489 Tierney, K., Wallace, W.A., & von Winterfeldt, D. (2003). A framework to quantitatively assess and
38 490 enhance the seismic resilience of communities. *Earthquake Spectra*, 19(4), 733-752.
- 41 491 Chandrasekaran, S., & Banerjee, S. (2016). Retrofit optimization for resilience enhancement of bridges
42 492 under multihazard scenario. *Journal of Structural Engineering*, 142(8), C4015012.
43 493 doi:10.1061/(ASCE)ST.1943-541X.0001396
- 46 494 Cimellaro, G., Reinhorn, A., & Bruneau, M. (2010). Framework for Analytical Quantification of Disaster
47 495 Resilience. *Engineering Structures*, 32, 3639–3649.
- 49 496 Cimellaro, G.P. (2016). *Urban resilience for emergency response and recovery. Fundamental Concepts and*
50 497 *Applications, Geotechnical, Geological and Earthquake Engineering*, 41, Springer International
51 498 Publishing, ISBN 978-3-319-30656-8.
- 53 499 Decò, A., Bocchini, P., & Frangopol, D. (2013). A probabilistic approach for the prediction of seismic
54 500 resilience of bridges. *Earthquake Engineering & Structural Dynamics* , 42, 1469-1487.
- 57 501 Dong, Y., & Frangopol, D. (2015). Risk and resilience assessment of bridges under mainshock and
58 502 aftershocks incorporating uncertainties. *Engineering Structures* , 83, 198-208.
- 59
60

- 1
2
3 503 Elms, D., McCahon, I. and Dewhurst, R. (2019). Improving infrastructure resilience. *Civil Engineering and*
4
5 504 *Environmental Systems*, 36(1), pp.83-99.
- 6 505 Elnashai, A., Borzi, B., & Vlachos, S. (2004). Deformation-based vulnerability functions for RC bridges.
7
8 506 *Structural Engineering Mechanics*, 17 (2), 215-244.
- 9 507 FEMA (2009). HAZUS - MH 2.1 Earthquake model technical manual. Washington, D.C.: Department of
10
11 508 Homeland Security, Mitigation Division.
- 12 509 Gidaris, I., Padjett, J., Barbosa, A., Chen, S., Cox, D., Webb, B., & Cerato, A. (2017). Multiple-hazard
13
14 510 fragility and restoration models of highway bridges for regional risk and resilience assessment in the
15
16 511 United States: state-of-the-art review. *Journal of Structural Engineering*, 143 (3).
- 17 512 Hayat, E., Haigh, R., & Amaratunga, D. (2019). A framework for reconstruction of road infrastructure after
18
19 513 a disaster. *International journal of disaster resilience in the built environment*.
- 20 514 Karamlou, A., & Bocchini, P. (2017). From component damage to system-level probabilistic restoration
21
22 515 functions for a damaged bridge. *Journal of Infrastructure Systems*, 23 (3).
- 23 516 Komendantova, N., Scolobig, A., Garcia-Aristizabal, A., Monfort, D., & Fleming, K. (2016). Multi-risk
24
25 517 approach and urban resilience. *International Journal of Disaster Resilience in the Built Environment*.
- 26 518 Mackie, K., & Stojadinovic, B. (2006). Post-earthquake functionality of highway overpass bridge.
27
28 519 *Earthquake Engineering and Structural Dynamics* , 35, 77-93.
- 29 520 Moschonas, I., Kappos, A., Panetsos, P., Papadopoulos, V., Makarios, T., & Thanopoulos, P. (2009).
30
31 521 Seismic fragility curves for greek bridges: methodology and case studies. *Bulletin of Earthquake*
32
33 522 *Engineering* , 7 (2), pp. 439-468.
- 34 523 Nakanishi, H., Black, J., & Matsuo, K. (2014). Disaster resilience in transportation: Japan earthquake and
35
36 524 tsunami 2011. *International Journal of Disaster Resilience in the Built Environment*.
- 37 525 Padgett, J., & DesRoches, R. (2007). Bridge functionality relationships for improved seismic risk
38
39 526 assessment of transportation networks. *Earthquake Spectra* , 23(1), 115-130.
- 40 527 Ptilakis, K., Riga, E., & Anastasiadis, A. (2013). New code site classification, amplification factors and
41
42 528 normalized response spectra based on a worldwide ground-motion database. *Bulletin of Earthquake*
43
44 529 *Engineering* , 11 (4), 925-966.
- 45 530 Rehak, D., Senovsky, P., Hromada, M., & Lovecek, T. (2019). Complex approach to assessing resilience
46
47 531 of critical infrastructure elements. *International Journal of Critical Infrastructure Protection*, 25, 125-
48
49 532 138.
- 50 533 Sgambi, L., Garavaglia, E., Basso, N., & Bontempi, F. (2014). Monte carlo simulation for seismic analysis
51
52 534 of a long span suspension bridge. *Engineering Structures*, 78, 100-111.
- 53 535 Sharma, N., Tabandeh, A., & Gardoni, P. (2018). Resilience analysis: A mathematical formulation to model
54
55 536 resilience of engineering systems. *Sustainable and Resilient Infrastructure*, 3(2), 49-67.
56
57 537 doi:10.1080/23789689.2017.1345257
- 58 538 Stefanidou S.P., & Kappos A. J. (2018). Bridge-specific fragility analysis: when is it really necessary?.
59
60 539 *Bulletin of Earthquake Engineering*, 1-36, <https://doi.org/10.1007/s10518-018-00525-9>.

- 1
2
3 540 Twumasi-Boakye, R., & Sobanjo, J. O. (2018). Resilience of regional transportation networks subjected to
4 hazard-induced bridge damages. *Journal of Transportation Engineering, Part A: Systems*, 144(10),
5 541 04018062.
6 542
7
8 543 Venkittaraman, A., & Banerjee, S. (2014). Enhancing resilience of highway bridges through seismic
9 retrofit. *Earthquake Engineering Structural Dynamics*, 43, 1173-1191.
10 544
11 545 Werner, S., Taylor, C., Cho, S., Lavoie, J., Huyck, C., Eitzel, C., et al. (2006). REDARS 2 Methodology
12 and software for seismic risk analysis of highway systems. Buffalo, New York, United States: (MCEER-
13 546 06-SP08).
14 547
15
16 548 Woessner, J., Danciu, L., Giardini, D., Crowley, H., Cotton, F., Grunthal, G., Valensise, G., Arvidsson, R.,
17 549 Basili, R., Demircioglu, M., Hiemar, S., Meletti, C., Musson, R., Rovida, A., Sesetyan, K., & Stucchi,
18 M. (2015) The 2013 European seismic hazard model: key components and results. *Bulleting of*
19 550 *Earthquake Engineering*, 13(12), 3553-3596. DOI 10.1007/s10518-015-9795-1
20 551
21
22 552 Zhang, W., Wang, N., & Nicholson, C. (2017). Resilience-based post-disaster recovery strategies for road-
23 bridge networks. *Structure and Infrastructure Engineering*, 13(11), 1404-1413.
24 553
25
26
27
28
29
30
31
32
33
34
35
36
37
38
39
40
41
42
43
44
45
46
47
48
49
50
51
52
53
54
55
56
57
58
59
60